Iran Polym J (2014) 23:289–296
DOI 10.1007/s13726-014-0224-0

ORIGINAL PAPER

Mechanical and barrier properties of XNBR-clay nanocomposite: a promising material for protective gloves

Mostafa Mirzaei Aliabadi · Ghasem Naderi · Seyed Jamaleddin Shahtaheri · Abbas Rahimi Forushani · Iraj Mohammadfam · Mehdi Jahangiri

Received: 24 July 2013 / Accepted: 20 January 2014 / Published online: 4 February 2014

Abstract Carboxylated nitrile butadiene rubber (XNBR)-based gloves are commonly used to protect users' hands from the aggressive environment in various industrial applications. Permeation resistance and mechanical properties of gloves should be simultaneously considered to accomplish adequate protection. Accordingly, in this study, XNBR was reinforced with different amounts of nanoclay and the resulting dispersion was examined using X-ray diffraction and transmission electron microscope. The results showed that, nanoclay has been appropriately dispersed in XNBR lattice and therefore, considerable enhancements in mechanical properties, including tensile strength and modulus were gained. The permeation resistance of the synthesized nanocomposites was studied by two solvents, including perchlorethylene and aniline with low and high affinity to XNBR, respectively. Using permeation test cell, parameters of breakthrough time (BT) and steady-state permeation rate (SSPR) were determined. The BT and SSPR of aniline in nanocomposites with 3 phr nanoclay in comparison with neat polymer were increased 89 % and decreased by 11 %, respectively. Degradation resistance test of nanocomposite demonstrated acceptable integrity of its barrier properties after repeated exposure to selected chemicals. Analysis of mechanical properties and permeation indices of synthesized nanocomposites illustrated that the application of these materials for manufacturing protective gloves seems promising.

Keywords Nanocomposites · Nanoclay · Chemical protective gloves · Mechanical properties · Permeation resistance

M. M. Aliabadi
Department of Occupational Health Engineering, School of Public Health, Tehran University of Medical Sciences, Tehran, Iran

G. Naderi
Iran Polymer and Petrochemical Institute, P.O. Box: 14965/115, Tehran, Iran

S. J. Shahtaheri (✉)
Department of Occupational Health Engineering, School of Public Health, Institute for Environmental Research, Tehran University of Medical Sciences, 14155-6446 Tehran, Iran
e-mail: shahtaheri@sina.tums.ac.ir

A. R. Forushani
Department of Biostatistics, School of Public Health, Tehran University of Medical Sciences, Tehran, Iran

I. Mohammadfam
Department of Occupational Health Engineering, Faculty of Health, Hamadan University of Medical Sciences, Hamadan, Iran

M. Jahangiri
Department of Occupational Health Engineering, School of Public Health and Nutrition, Shiraz University of Medical Sciences, Shiraz, Iran

Introduction

Skin is the second most common route by which the hazardous chemicals can enter into the human body in occupational settings [1]. The main locations of exposure are both hands and forearms, which are typically engaged during different industrial routine activities [2]. Chemical protective gloves (CPGs), as a subset of personal protective equipment (PPE), are one of the last items in the hierarchy of hazard control measures. Therefore, their usage in many workplaces is indispensable [3]. The primary objective of CPGs' application is preventing or reducing skin contact with potentially hazardous chemicals. However, in some

circumstances, the permeation of hazardous chemicals through CPGs might reduce the degree of protection. Unfortunately, the permeation of chemicals into the CPGs can occur without the knowledge of the users, since there is no evidence of visible damage to the material [4]. The migration of penetrant molecules into the materials of glove is the driving mechanism that causes the permeation. The later release of penetrant molecules from the interior surface of the gloves appears in the form of vapor [5].

There are two indices to decide about the permeation resistance of gloves; breakthrough time (BT) and permeation rate [6]. The time required for the penetrant molecules to appear on the opposite side of the gloves is called the BT. Permeation rate is equal to the mass of penetrant molecules passing through the surface area of the gloves material (in terms of microgram/cm^2 min). The steady-state permeation rate (SSPR) would be calculated whenever all forces that determine permeation process reach a dynamic equilibrium and permeation rate does not change anymore [7].

The efficacy of gloves against hazardous chemicals should be evaluated from two points of view; chemically and physically (mechanically). Permeation resistance is considered as a chemical property, whereas both tensile strength and degradation resistance are important parameters in mechanical evaluations [7]. In other words, although the permeation resistance is a vital parameter in selection of protective gloves, the mechanical properties such as tensile strength and modulus should not be sacrificed in favor of the permeation resistance [7]. Tensile strength is defined as the force (in terms of megapascal) needed to stretch a glove sample as long as it ruptures. The amount of force at 100, 200 and 300 % elongation called modulus at 100, 200 and 300 % (hereafter M100, M200 and M300), expresses the magnitude of force needed to pull a glove sample to one-fold, two-fold, and three-fold of its length, respectively.

Regarding mechanical properties of CPGs, tensile strength is related to extreme use condition of gloves, whereas, M300 is more associated with normal use condition, i.e. normal hand mobility in occupational task.

Layered silicates-polymer nanocomposites, as a new class of materials, have recently drawn considerable attention due to their impressive enhancement of barrier [8, 9] and mechanical properties [10, 11] of a polymer. Layered silicates are considered to have a large aspect ratio and be intrinsically impenetrable. Therefore, if they become well dispersed in a polymer matrix, it creates a tortuous path; increasing the effective route length of solvent molecules for diffusion [12, 13]. To the best of our knowledge, literature search revealed an absolute shortage of publication on producing and characterization of dipping goods such as gloves from nanocomposite. The main focus of this research is therefore devoted to preparation and mechanochemical characterization of carboxylated nitrile butadiene rubber (XNBR)-clay nanocomposite as CPGs for the first time. Furthermore, degradation resistance of nanocomposite gloves has been tested under simulation of use conditions (simulated conditions).

Experimental

Materials

The XNBR lattice used in this research was commercialized Synthomer 6617 and was kindly supplied by the Synthomer Company (Malaysia). Compounding ingredients such as zinc oxide was obtained from Pars Oxide Parto Iran, sulfur was provided by Iran Tesdak Co., zinc diethyldithiocarbamate (ZDEC) and potassium hydroxide were supplied by Merck (Germany). Aromatic polyglycol ether (Emulvin WA), as an emulsifying, stabilizing and wetting agents for lattices was provided by Lanxess, Germany. Perchlorethylene, also known as PERC (solubility parameter, 19 MPa$^{1/2}$), and aniline (solubility parameter, 21.1 MPa$^{1/2}$) were purchased from Merck Company (Germany). Pristine sodium montmorillonite (Cloisite Na$^+$), with a cationic exchange capacity (CEC) of 92.6 mequiv/100 g, was obtained from Southern Clay Products, Texas, USA. Polydimethylsiloxan (PDMS) solid phase microextraction (SPME) fibers with manual holder were supplied from Supelco (Bellefonte, PA, USA).

Compounding and sample preparation

The preparation of XNBR–clay nanocomposites together with an explanation for each step is schematically shown in Fig. 1a, b. Initially, Cloisite Na$^+$ was dispersed in water with a mechanical stirrer at a ratio of 5/95. The pH of this dispersion was adjusted to the pH of XNBR lattices by adding the required amount of potassium hydroxide (KOH) aqueous solution. In order to prevent the lattices from coagulating upon adding clay, sufficient amount of Emulvin WA was also added into the aqueous dispersion of clay and the resulting mixture was vigorously stirred for a period of time. Then, the as-prepared clay aqueous dispersion was incorporated into the XNBR lattice, and the mixture was stirred continuously using a magnetic stirrer at room temperature for a period of 24 h. The concentration of clays varied from 3 phr (parts per hundred of rubber) to 6 and 9 phr. In a parallel way, ball milling of ingredients functioning as curatives were conducted and the obtained dispersions were added to the XNBR nanocomposite. Subsequently, the entire mixture was stirred for another 24 h and finally, XNBR–clay nanocomposite lattices were obtained. Afterward, XNBR-nanocomposite lattices were

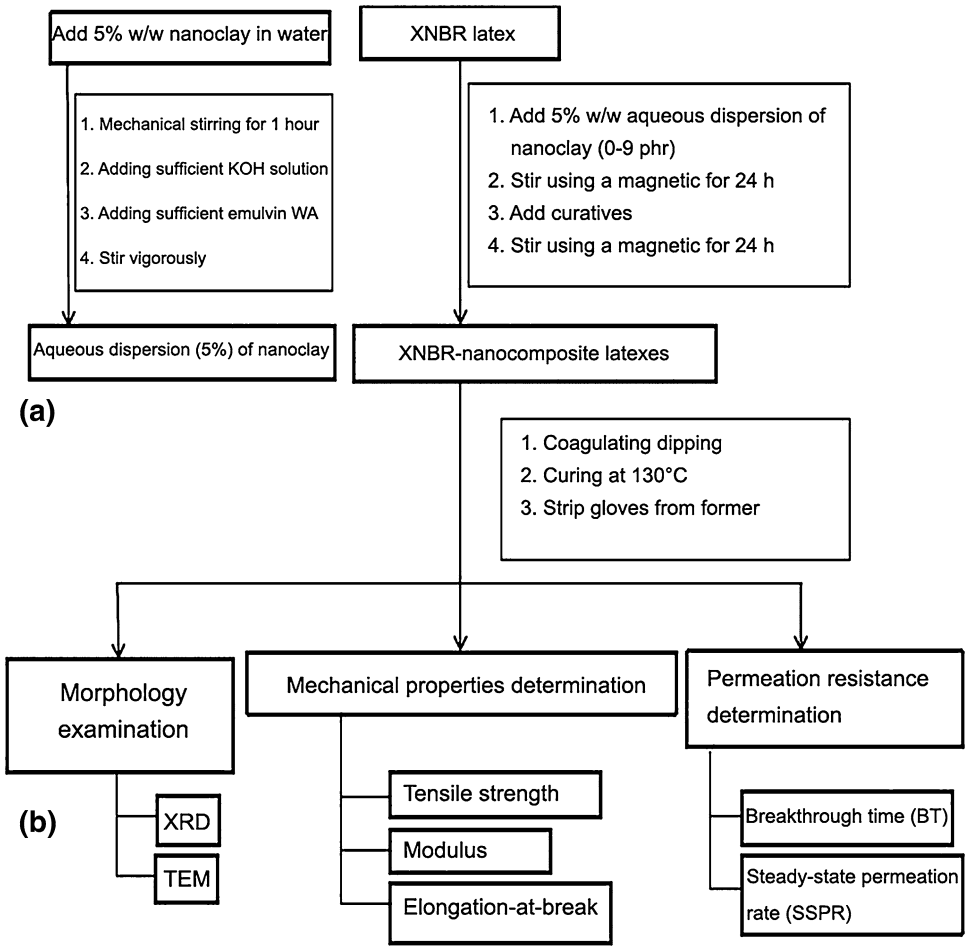

Fig. 1 The schematic diagram of the experiment for preparing: **a** aqueous dispersion of nanoclay and **b** XNBR-nanocomposite lattices and curing films and characterizations

used to prepare the nanocomposite vulcanisates by coagulation dipping using former gloves. In this process, the former glove was dipped in 40 % calcium nitrate solution (as coagulant) for 15 s and then it was dried at 100 °C for 3 min and cooled to temperatures below 65 °C. Afterward; the former treated coagulant was dipped into the XNBR-nanocomposite lattices and remained for 1 min. The sample was allowed to be gelled at room temperature for 3 min and was leached with water at 45 °C. Finally, the dipped samples were cured in a hot air oven at 130 °C.

In a convenient notation, samples were denoted as $XNBR_{Na}$, where the subscript Na indicates the amount of Cloisite Na^+ used (0, 3, 6, and 9 phr). Thus, $XNBR_3$ represents XNBR- nanocomposite having a nanoclay loading of 3 phr.

Characterization methods

X-Ray diffraction analysis

The change in the gallery spacing, i.e. the spacing of the layered silicates, is calculated using the Bragg's Law (Eq. 1) considering the peak position in the X-Ray diffraction (XRD) pattern:

$$d = n\lambda/2\sin\theta \quad (1)$$

where d is the gallery spacing, n is an integer, λ is the wavelength of the X-ray (for Cu-target used here, the value of λ is 0.154 nm), and θ is the angle of diffraction.

Transmission electron microscopy

Transmission electron microscopy (TEM) observations of the nanocomposite samples were carried out by a Philips TEM (CM30-TEM), using an acceleration voltage of 200 kV. The TEM specimens were prepared by ultra cryo-microtomy equipped with a diamond knife at −100 °C.

Mechanical properties

The mechanical (tensile) properties of vuclanizates were determined using Instron 8511. For this measurement, dumb-bell specimens were punched out from vulcanized nanocomposite film using a type C die. The tests were

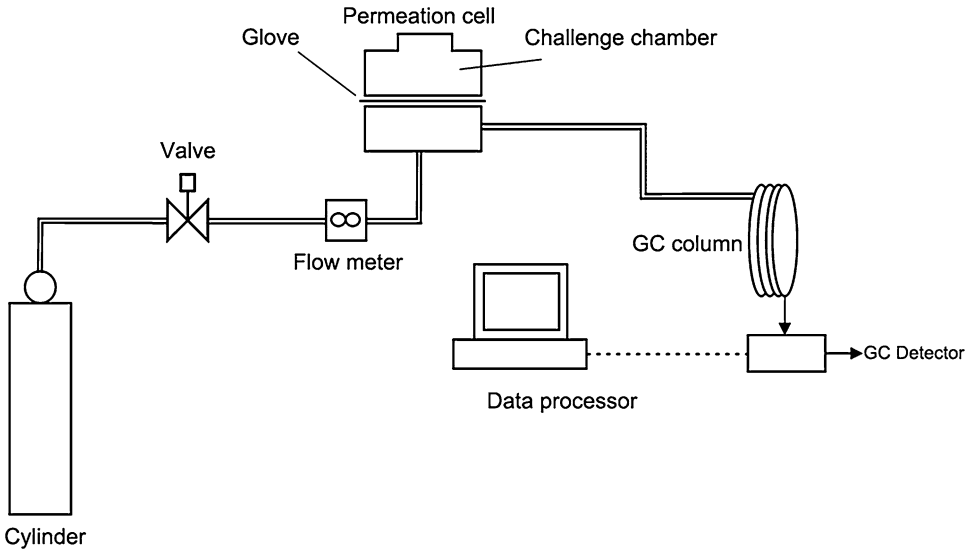

Fig. 2 Experimental system of open loop permeation cell with related accessories

performed according to ASTM D 412-98 at a cross-head speed of 500 mm/min at room temperature. Tensile strength, elongation-at-break and modulus were recorded.

Permeation properties

The continuous contact permeation test was carried out in accordance with ISO 6529:2001 with an open-loop configuration. (Fig 2) illustrates the sketch of the experimental setup together with its related accessories. A two-chambered test cell with a circular exposure area of 4.9 cm^2 was used to expose the nanocomposite specimens to the challenge solvents. Samples were located between two PTEF gaskets, while the vulcanized XNBR-nanocomposite separated the challenge and collection side of the permeation cell. The test was commenced by charging the challenge solvents to the upper chamber (challenge side). When the test begins, the solvent diffuses at the molecular level through the nanocomposite sample and evaporates from the interior surface. The collection side of the cell was purged with nitrogen, as a collection medium, with a flow rate of approximately 85 mL/min. During the experimental run, discrete samples were taken from the downstream sampling point every 7 min with an Solid-phase microextraction (SPME) fiber [14, 15] followed by gas chromatography analysis (Varian CP-3800) equipped with a flame-ionization detector (GC-FID). SPME is a simple, practical, solventless and sensitive technique for determination of organic compounds. The permeation cell, and all related accessories were connected with Teflon tubing. Samples, solvents, and equipments were kept at room temperature during the all permeation test runs. All tests were conducted in triplicate for any sample-solvent combinations. Therefore, the permeation indices presented in this study are averaged values from at least three runs.

The thickness of each sample was measured to the nearest 0.01 mm with a micrometer screw gauge taken at five locations across the sample. The average thickness of nanocomposite samples was 0.35 ± 0.02 mm. The difference in samples thicknesses was not significant.

In order to calculate the permeation rate J (μg/cm^2 min) of each solvent, Eq. 2 was used [16]:

$$J = \frac{F \times C}{A} \quad (2)$$

where F is the flow rate of nitrogen (85 mL/min), C is the concentration of the challenge solvent in the collection medium at time t (μg/mL), A is the exposed surface area of gloves' materials to the solvent (4.9 cm^2).

In the present study, BR was defined as the time required for J to reach 1 μg/cm^2 min value. The SSPR was identified by prolonged constant permeation rate.

Degradation resistance testing

Successive cycles of exposure/decontamination of gloves' materials with chemicals can change the protection afforded by the gloves [17]. Since changes in tensile strength are considered as an indicator of polymer degradation, to examine the possible degradation of nanocomposite due to the increasing number of exposure/decontamination cycles, the variations in tensile properties were measured up to maximum 10 cycles. In order to perform this experiment, the apparatus and protocol mentioned by Gao was used [18]. In practice, the test specimen (a 17.5 cm circular section of the nanocomposite), as a membrane, was placed between two 15-cm-diameter pipe stub ends. The pipe stub

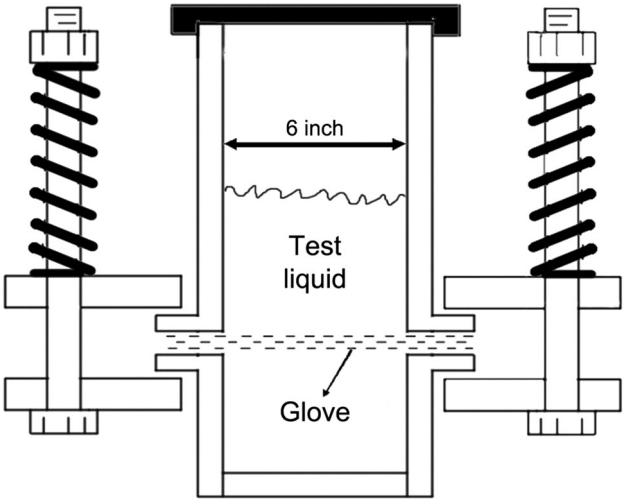

Fig. 3 Contamination apparatus

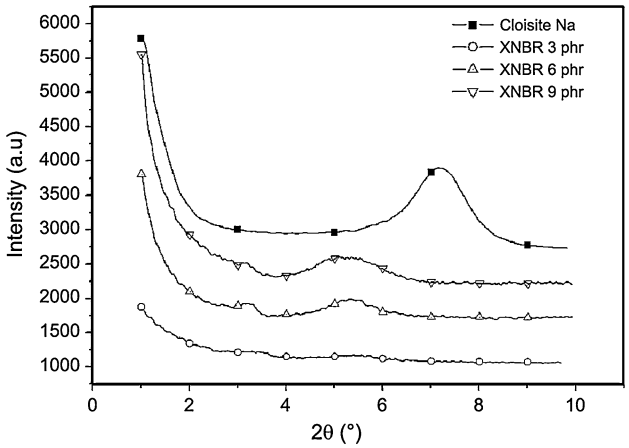

Fig. 4 XRD diffractograms of Cloisite Na^+ and nanocomposite films having different amounts of nanoclay

ends were lightly compressed between two flanges to make a gas-tight seal (Fig. 3). The timer was started as soon as a sufficient amount of the test chemical was added to the top compartment of the apparatus. After reaching steady state permeation, which was determined by our already permeation test, the sample was removed and placed into a hot-air oven for 24 h at 100 °C for decontamination. To perform this process, 22 circular samples of $XNBR_3$ nanocomposite with a diameter of 17.5 cm were prepared on the first day. Two samples were randomly selected from 22 samples and punched into 6 dumb-bell specimens and tensile strengths were measured. The results of this test represent the baseline (new samples) values of the tensile strength. The remained 20 samples were exposed to aniline using the mentioned apparatus and then thermally decontaminated as explained above. Afterward, 2 of these 20 remained samples were randomly selected and punched into 6 dumb-bell specimens. The results of tensile strength that were obtained from testing of the two samples represent the first exposure/decontamination cycle values. For the remaining 18 samples, the same exposure/decontamination cycles were repeated. On the next day, another two samples were randomly selected again, and the protocols were applied to the remaining samples and so on.

Results and discussion

Morphology

X-Ray diffraction is a useful technique for monitoring of layered silicates and polymer nanocomposite. The XRD of Cloisite Na^+ and vulcanized nanocomposites films are given in Fig. 4. Cloisite Na^+ shows a single peak at $2\theta = 7.17$, which corresponds to the basal spacing of 1.23 nm. For XNBR–clay nanocomposite, the characteristic diffraction peak shifts to the lower 2θ with respect to that of nanoclay. Vulcanized nanocomposites samples containing 3, 6, and 9 phr of nanoclay show peaks at a *d* spacing of 2.57, 1.64 and 1.58 nm, respectively. This shows that, the chains of XNBR are entered into the galleries of the nanoclay, resulting in an increase in *d* spacing of the nanoclay, which is appearing from the shift of 2θ value towards the lower angle. In $XNBR_3$ sample, the disappearance of the diffraction peak indicates that the silicate layers are uniformly and completely dispersed in the polymer matrix.

TEM is the most important technique to visualize the dispersion of layered silicate in the polymer matrix. TEM images of the XNBR–clay nanocomposite for different nanoclay contents (3, 6, and 9 phr) are depicted in Fig. 5a, b. The dark lines in TEM images depict the dispersion of silicates in the polymer matrix. As can be seen in the $XNBR_3$ specimen (Fig. 5a), exfoliated layered silicates were uniformly dispersed in the polymer matrix. Although with the increases in percentage of nanoclay to 9 phr the dispersion decreases and nanoclays are aggregated (Fig. 5b). The TEM results were in agreement with the XRD results.

Mechanical properties of nanocomposites

The mechanical properties of XNBR nanocomposites, containing different amounts of nanoclay, are tabulated in (Table 1). Compared to the neat polymer $XNBR_0$, compounds of $XNBR_3$ and $XNBR_6$ show 39 and 65 % increase in tensile strength, and 20 and 64 % increase in the value of M300, respectively. The degree of dispersion of filler in rubber matrix and the intensity of interaction between rubber chain and filler critically influence the degree of enhancement in mechanical properties of nanocomposites.

The observed enhancement of the mechanical properties is attributed to the high aspect ratio and rigidity of nanoclay as well as to great interfacial interactions of rubber and nanoclay. Moreover, this behavior may be explained by nanoconfinement of rubber chains on the filler surface. Consequently, it increases the effective surface area of filler and creates strong rubber-filler interactions [19]. Obviously, these phenomena occur in the presence of exquisite dispersion of filler, which clearly is a logical assumption for the present case as confirmed by the results of XRD and TEM.

Considering the value of M300 as a criterion of flexibility of industrial gloves, which should be around 10 MPa, it is found that there is a constraint in using more than 3 phr nanoclay due to the undesirable increase of the value of M300 for samples having more than 3 phr. In other words, quantity of nanocaly employed to improve the barrier properties of protective gloves should be tuned according to the various considered properties [20]. The reinforcing effect of filler is also illustrated by the increase in the ratio of modulus at 100 % elongation of filled samples (M_{100f}) to that of neat XNBR (M_{100n}).

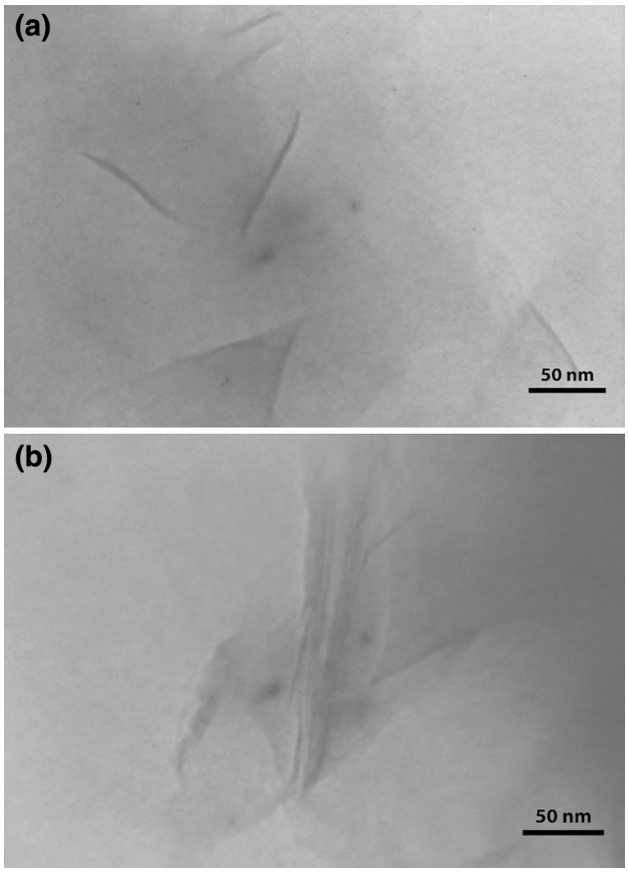

Fig. 5 TEM images of the XNBR–clay nanocomposites at: **a** 3 ($XNBR_3$) phr and **b** 9 ($XNBR_9$) phr loading

Permeation properties of the nanocomposites

The permeation indices of PERC and aniline thorough XNBR–clay nanocomposites at different nanoclay loadings were determined using the permeation test cell as illustrated in Fig. 6. The measured values of permeation indices were analyzed from statistical significance ($p < 0.05$) point of view, using analysis of variance (ANOVA), in order to realize whether the nanoclay has affected the permeation resistance.

It can be seen in Fig. 6 that the value of BT increases in the presence of nanofilled samples compared to the neat polymer, whereas the value of SSPR decreases. The former can be explainable by considering a tortuous zigzag path created by clay nanolayers that enforce the solvent molecule to bypass impenetrable silicate layered and thereby increasing the traveled distance (Fig. 7). In addition, based on the nanoconfinement concept, restricted mobility of the rubber chain in the presence of clay may be accounted for by increases in BT. The reduction of SSPR may be explained in terms of the reduced volume fraction of permeable polymer in the presence of impenetrable silicate layered, i.e. reduction of an available cross-sectional area for diffusion. In other words, reduced SSPR can be attributed to the reduction in the solubility. However, the extent to which these permeation indices are affected by adding nanoclay is a function of the difference of solubility parameters (between neat polymer and permeant solvent) and amount of filler.

The permeation indices of relatively lesser susceptibility for permeating, i.e. PERC (because of the closeness of solubility parameter of the solvent and the polymer to each other) through the nanocomposites at different loadings of

Table 1 Mechanical properties of XNBR nanocomposite

Name	Tensile strength (MPa)	Elongation-at-break (%)	M100 (MPa)	M200 (MPa)	M300 (MPa)	M_{100f}/M_{100n}
$XNBR_0$	30	489	3.7	6.3	9.4	1
$XNBR_3$	41.7	500	4.9	8.3	11.3	1.32
$XNBR_6$	49.3	520	5.8	10	15.4	1.56
$XNBR_9$	57	530	14.5	19	23.9	3.91

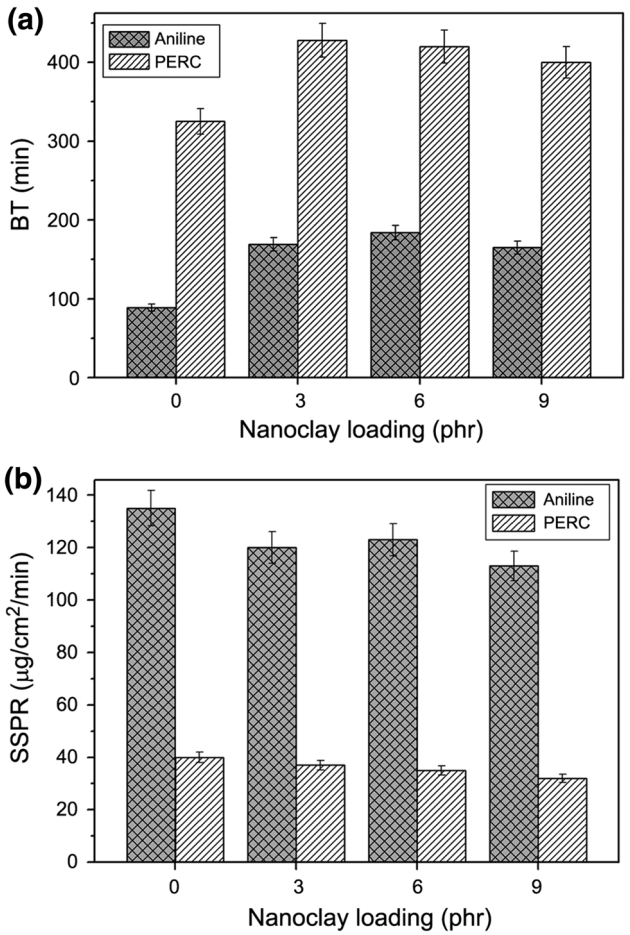

Fig. 6 **a** Breakthrough time (BT) and **b** SSPR for selected solvent thorough XNBR–clay nanocomposites at different nanoclay loadings

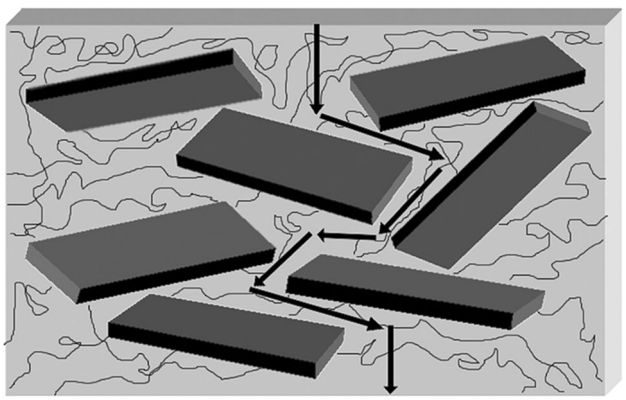

Fig. 7 Schematic representation of how tortuous path can longer the traveled distance of solvent molecules through the nanocomposite

nanoclay are shown in Fig. 6. BT value tends to be increased up to 3 phr with increase in filler loading. However, beyond which it decreases. Indeed, the aggregation of filler at higher loading is possibly initiated, as confirmed in XRD diffractograms and TEM images, and accordingly, the interaction of polymer-filler drops and the number of obstacles against the molecules of solvent decreases. In case of $XNBR_3$ (the convenient ones for producing gloves at commercial scale regarding M300 value), BT increased from 325 min ($XNBR_0$) to 428 min, i.e. the increase was more than 30 % compared to the neat polymer. The values of SSPR show a decrease with filler loading. With increase of filler loading, the values of SSPR tend to decrease by the factor of 20 % on going to 9 phr. The SSPR of $XNBR_3$ is decreased from 40 μg/cm^2/min ($XNBR_0$) to 37 μg/cm^2/min, i.e. the decrease of 7.5 % compared to the neat polymer.

A similar trend was observed for permeation indices of aniline with relatively higher susceptibility for permeating, but with a different magnitude (Fig. 6). The BT and SSPR of aniline in neat polymer are shorter and higher, respectively compared to the corresponding values of PERC. This discrepancy can be attributed to the difference in solubility parameter of the solvent and the polymer. The solubility parameter of PERC, aniline and the polymer are 19, 21.1 and 20.5 MPa$^{1/2}$, respectively. This difference is lower (0.6 MPa$^{1/2}$) for aniline relative to the PERC (1.5 MPa$^{1/2}$). In case of $XNBR_3$, BT increased from 89 min ($XNBR_0$) to 169 min, i.e. BT increased more than 89 % and SSPR decreased from 135 μg/cm^2/min ($XNBR_0$) to 120 μg/cm^2/min, i.e. SSPR decreased more than 11 % compared to the neat polymer ($XNBR_0$). It can be concluded that, adding nanoclay to XNBR changes the permeation indices of aniline more than the same indices in PERC in desirable trends. This discrepancy is owing to a strong hydrogen-bonding tendency of aniline and hydrophilic features of the surface of nanoclay that induce strong interaction between aniline and vulcanizate [12, 21].

Degradation resistance testing

According to ASTM D-412, degradation is defined as the change in tensile strength of the material as the result of repeated chemical exposure. In addition, maintenance and thermal decontamination are required practices for CPGs in industry. Since $XNBR_3$ nanocomposite is desirable for producing gloves and aniline permeation indices demonstrate more improvement, this chemical-nanocomposite pair was selected for degradation resistance testing. (Fig 8) depicts the change in tensile strength of $XNBR_3$ nanocomposite against aniline after exposure/decontamination cycles. The tensile strength of the new sample and after 5 and 10 exposure/decontamination cycles were 42, 41 and 39 MPa, respectively. In comparison with the new sample, after 10 exposure/decontamination cycles, nanocomposites lost on average 4.8 and 6.5 % of their original tensile strength. As it can be seen in Fig. 8, the losses occur mainly in the first exposure/decontamination cycle. This

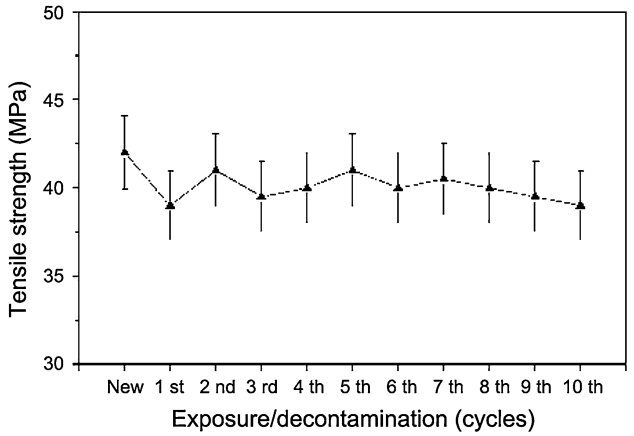

Fig. 8 Change in tensile strength of $XNBR_3$ nanocomposite against aniline after exposure/decontamination cycles

may be due to the immature cure of the polymer. Since a relationship exists between the heat and the time of cure, the decontamination heat may cause more polymer cure. Nevertheless, tensile strength stays statistically ($p > 0.05$) stable after the first cycle. The degradation resistance of nanocomposite maintains virtually after repeated exposure to chemicals. Degradation resistance testing demonstrates a negligible change in mechanical properties of nanocomposite after repeated exposure to the selected chemical.

Conclusion

XNBR nanocomposites were prepared using Cloisite Na^+ as nanofiller in different loadings (3, 6 and 9 phr). Mechanical properties such as tensile strength and modulus increased substantially by adding nanoclay up to 9 phr, as compared to the neat polymer. Since the value of modulus at 300 % elongation is a criterion of flexibility of protective gloves and should be around 10 MPa, and this value is 11.3 MPa in the case of $XNBR_3$, it was found that, the maximum nanoclay loading for this purpose should be 3 phr. Additionally, this nanocomposite showed superior permeation resistance against the aniline and PERC solvents, compared to those of the neat polymer. However, the extent of this enhancement was influenced by the solubility parameter differences of polymer and solvents as well as an amount of filler. Degradation resistance testing of nanocomposite demonstrated the acceptable integrity of the barrier after repeated exposure to selected chemical.

Acknowledgments This research has been supported by Tehran University of Medical Sciences and Health Services grant (project no. 19570-27-03-91). Also, the supports received by Iran Polymer and Petrochemical Institute are highly appreciated. Also, the authors would like to express appreciation to Siau Woon Wang from Synthomer Company for effective assistant.

References

1. Chao KP, Wang P, Chen CP, Tang PY (2011) Assessment of skin exposure to *N,N*-dimethylformamide and methyl ethylketone through chemical protective gloves and decontamination of gloves for reuse purposes. Sci Total Environ 409:1024–1032
2. Berardinelli SP (1988) Prevention of occupational skin disease through use of chemical protective gloves. Dermatol Clin 6:115–119
3. Forsberg K (2011) In: Patty's Industrial Hygiene, John Wiley, 1235-1262
4. Boman A (2012) In: Kanerva's Occupational Dermatology, Springer, 1225-1234
5. Chao KP, Lee PH, Wu MJ (2003) Organic solvents permeation through protective nitrile gloves. J Hazard Mater 99:191–201
6. Anna DH (2003) Chemical protective clothing. AIHA Press, Fairfax
7. Boman A, Estlander T, Wahlberg JE (2004) Protective gloves for occupational use. CRC, Boca Raton
8. Maiti M, Bhowmick AK (2007) Effect of polymer-clay interaction on solvent transport behavior of fluoroelastomer–clay nanocomposites and prediction of aspect ratio of nanoclay. J Appl Polym Sci 105:435–445
9. Krzemińska S, Rzymski W (2009) Effect of layered silicate on the barrier properties of cured butyl rubber. Int J Phys Conf Series 012007
10. Luo JJ, Daniel IM (2003) Characterization and modeling of mechanical behavior of polymer/clay nanocomposites. Compos Sci Technol 63:1607–1616
11. Yousefi AA (2011) Hybrid polyvinylidene fluoride/nanoclay/MWCNT nanocomposites: PVDF crystalline transformation. Iran Polym J 20:725–733
12. Sridhar V, Tripathy DK (2006) Barrier properties of chlorobutyl nanoclay composites. J Appl Polym Sci 101:3630–3637
13. Saritha A, Joseph K, Thomas S, Muraleekrishnan R (2012) Chlorobutyl rubber nanocomposites as effective gas and VOC barrier materials. Compos Part A: Appl Sci Manufac 43:864–870
14. Chao KP, Wang VS, Hong GM (2012) Development of an in-cell SPME method to determine the chemical resistance of polymeric membranes to permeation by organic solvents. Polym Test 31:1–6
15. Zare Sakhvidi MJ, Bahrami AR, Ghiasvand A, Mahjub H, Tuduri L (2013) SPME-based air sampling method for inhalation exposure assessment studies: case study on perchlorethylene exposure in dry cleaning. Environ Monit Assess 185:1–9
16. Jamke RA (1989) Understanding and using chemical permeation data in the selection of chemical protective clothing. In: Perkins JL, Stull JO (eds) Chemical protective clothing performance in chemical emergency response, ASTM STP 1037. Am Soc Test Mater, Philadelphia, pp 11–22
17. Gao P, Tomasovic B, Stein L (2011) Performance evaluation of 26 combinations of chemical protective clothing materials and chemicals after repeated exposures and decontaminations. J Occup Environ Hyg 8:625–635
18. Gao P, Tomasovic B (2005) Change in tensile properties of neoprene and nitrile gloves after repeated exposures to acetone and thermal decontamination. J Occup Environ Hyg 2:543–552
19. Chen K, Wilkie CA, Vyazovkin S (2007) Nanoconfinement revealed in degradation and relaxation studies of two structurally different polystyrene–clay systems. J Phys Chem B 111:12685–12692
20. Palakattukunnel ST, Thomas S, Sreekumar P, Bandyopadhyay S (2011) Poly(ethylene-*co*-vinyl acetate)/calcium phosphate nanocomposites: contact angle, diffusion and gas permeability studies. J Polym Res 18:1277–1285
21. Saritha A, Joseph K, Boudenne A, Thomas S (2011) Mechanical, thermophysical, and diffusion properties of TiO_2-filled chlorobutyl rubber composites. Polym Compos 32:1681–1687